Quarterly Report: Work Completed 3-31-2010

Methane Recovery from Hydrate-bearing Sediments

Funding Number: DE-FC26-06NT42963

Submitted By:

J. Carlos Santamarina
Georgia Institute of Technology
School of Civil and Environmental Engineering
Atlanta, GA 30332-0355
Phone: (404)-894.7605
Fax: (404)-894.2278
E-mail: jcs@gatech.edu

Costas Tsouris
Oak Ridge National Laboratory
Georgia Institute of Technology
School of Civil and Environmental Engineering
Atlanta, GA 30332-0373
E-mail: costas.tsouris@ce.gatech.edu

Acknowledgment: This material is based upon work supported by the Department of Energy under Award Number DE-FC26-06NT42963

INTRODUCTION - ANTICIPATED MAIN RESULTS

Goals: Identifying, understanding and modeling processes involved in methane production from hydrate-bearing sediments.

Approach: observation and interpretation of phenomena at multiple scales, ranging from the pore-contact scale to the macro-reservoir scale, taking into consideration various possible driving forces (e.g., depressurization, thermal stimulation).

Anticipated results and most significant contributions: In view of our experience accumulated since the beginning of the project, we anticipate that some of the main results from this study will address:

- *Hydrate formation and growth*. Different conditions (unsaturated from gas phase, from ice, from dissolved phase, in water-wet and oil-wet sediments, during gas exchange). Formation rates at gas-water interface. Transients. Spatial distribution. *Relevance to marine and permafrost environments*.
- *Hydrate-mineral bonding and tensile strength*. Implications on the mechanical behavior of hydrate-bearing sediments in view of production strategies
- *Gas production by heating and depressurization*. Study in 5-m long 1-D cell. Experimental study and modeling
- *Gas production by chemo-driven methods*. Fundamental understanding of CO_2-CH_4 exchange
- *Gas production by transients*
- *The role of effective stress* in formation and production
- *Gas invasion versus gas production* – Evolution of degree of saturation and fluid conduction. Fluid-driven fractures
- *Fluid conductivity in spatially varying sediments*
- *Thermodynamic formulation*
- *Coupled thermo-hydro-chemo-mechanical formulation*
- *Production strategies in different formations*
- *Relevance to real systems*

Research Team: Shin graduated and moved to Korea (Assistant Professor). Espinoza is now fully dedicated is completing the study on contact angle and surface tension. A visiting scholar L. Velasco (PhD at U. Andes) has joined the effort for this 2010 year.

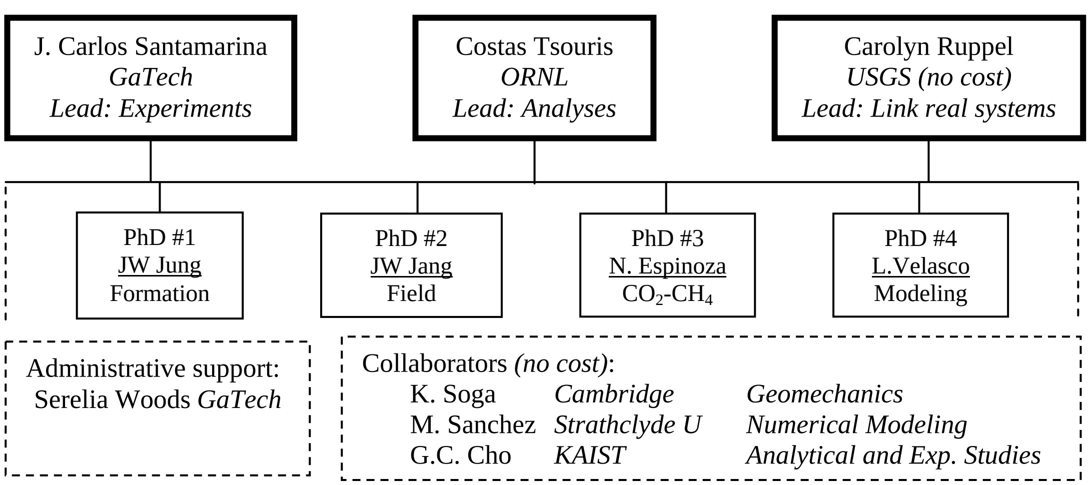

SUMMARY OF RESEARCH DEVELOPMENTS DURING THIS QUARTER

During this quarter, the research team has been dedicated to completing test sequences, advancing analyses, and preparing manuscripts for all tasks reported in previous quarterly reports. The most relevant themes have included:

- Hydrate growth, induction time, supercooling, vibration effects
- Spatial variability effects
- CO_2-CH_4 replacement
- Coupled thermo-hydro-chemo-mechanical modeling
- Methane production studies using the ORNL Seafloor Process Simulator (SPS)
- Field conditions

This report documents the latest test conducted with the ORNL SPS device. The test configuration of the Georgia Tech chamber in the ORNL SPS is shown in the diagrams below.

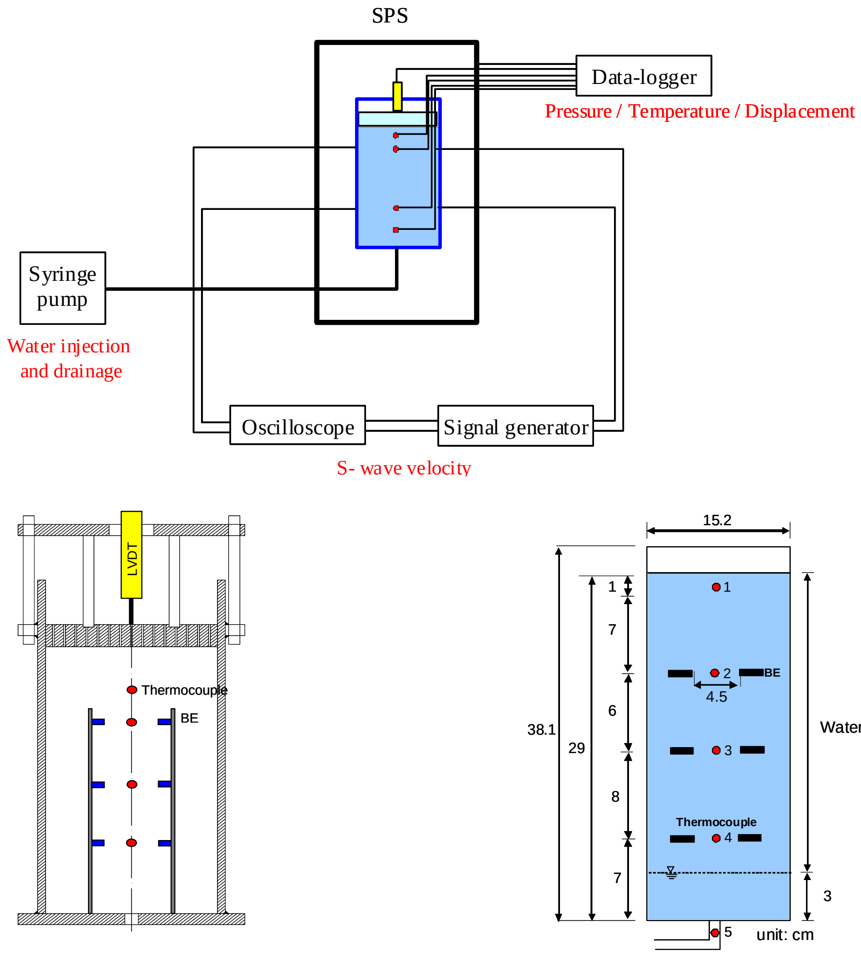

Effective stress cell ~up to 130kPa

Spring constant: 306N/cm

Cylinder ID 15.2cm, Length 38.1cm

Measurement: S-wave velocity, temperature (4), displacement

Figure 1. Schematic diagram of the test chamber in the ORNL SPS.

The most recent test with the ORNL SPS vessel documented here is a continuation of the tests described in a previous report: “Quarterly, Fall 2009”. The experimental conditions of the most recent test are summarized in the following table, while the preparation steps for the test chamber are shown sequentially in the images of Figure 2 (see next page).

	Measurements	**Soil Type**	**Procedure**
Test 4	Pressure (2) Temperature (6) S-wave (3 Pairs) Volume change	F80 (sieved by #140) + kaolinite (3% mass ratio)	Setup the chamber Adjust soil saturation at 35% Pressurize and cool down the chamber First water injection and drainage Second salty water injection and drainage Depressurize

Specimen formation and instrumentation (Test #4)

Figure 2. Preparation of the test chamber for the experiment.

Hydrate Formation

Hydrate is formed using the unsaturated soil method. During formation, the gas pressure drops and heat is released. Figure 3 below shows the PT evolution for Test #4.

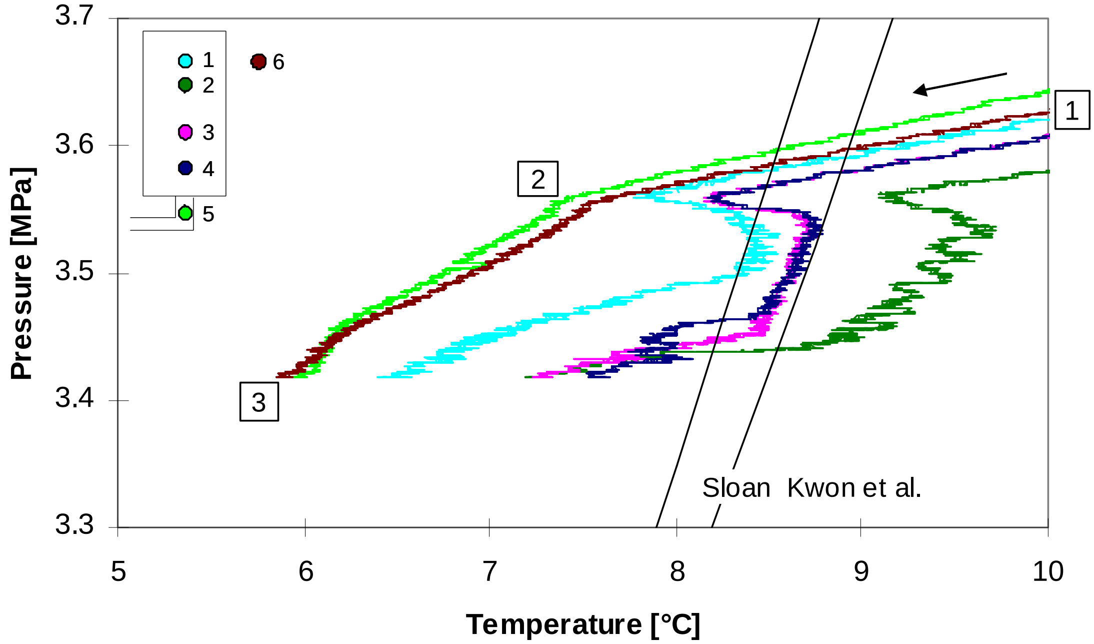

Figure 3. Pressure and temperature history during hydrate formation:
the temperature decreases from 1 to 3.

Water injection/drainage cycle

Additional hydrate forms during water injection and drainage. This phenomenon was also observed in previous tests, as well as the fact that some hydrate dissolution occurs during water injection due to the low concentration of CO_2 in the injected water that was kept at room conditions.

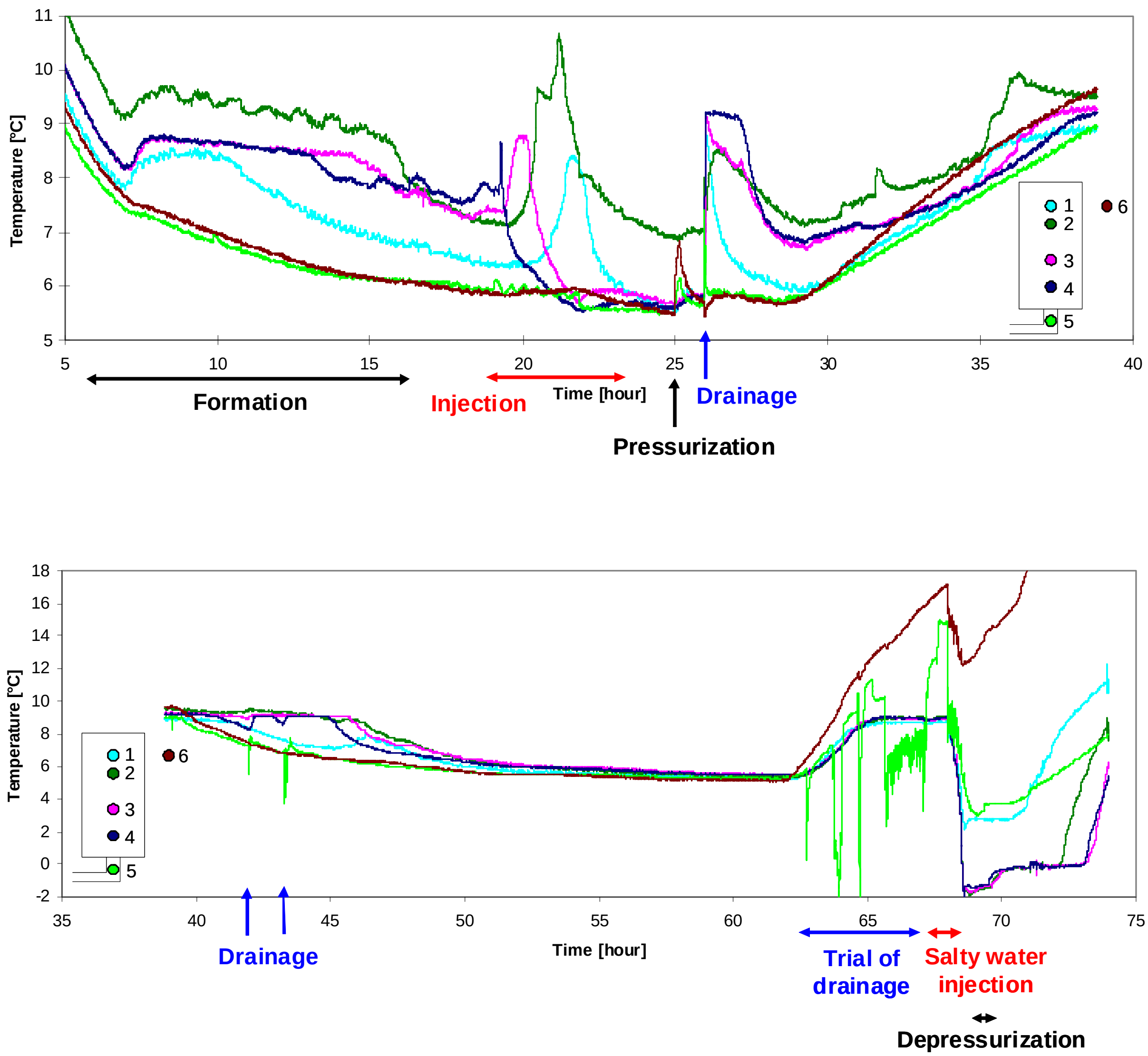

Figure 4. Temperature history during the test.

Amount of hydrate formation P-T Analysis

The modified Peng-Robinson equation of state [Stryjek and Vera, 1986] has been used to calculate the gas pressure and volume dependency on temperature.

$$P = \frac{RT}{V-b} - \frac{a}{V(V+b)+b(V-b)} \qquad \textit{modified Peng-Robinson (PRSV)}$$

The solubility of CO_2 in the non-hydrate region is calculated by the equation of Duan and Sun (2003).

- Amount of hydrate formed during overnight (1st day) under unsaturated condition (S_w=35%)

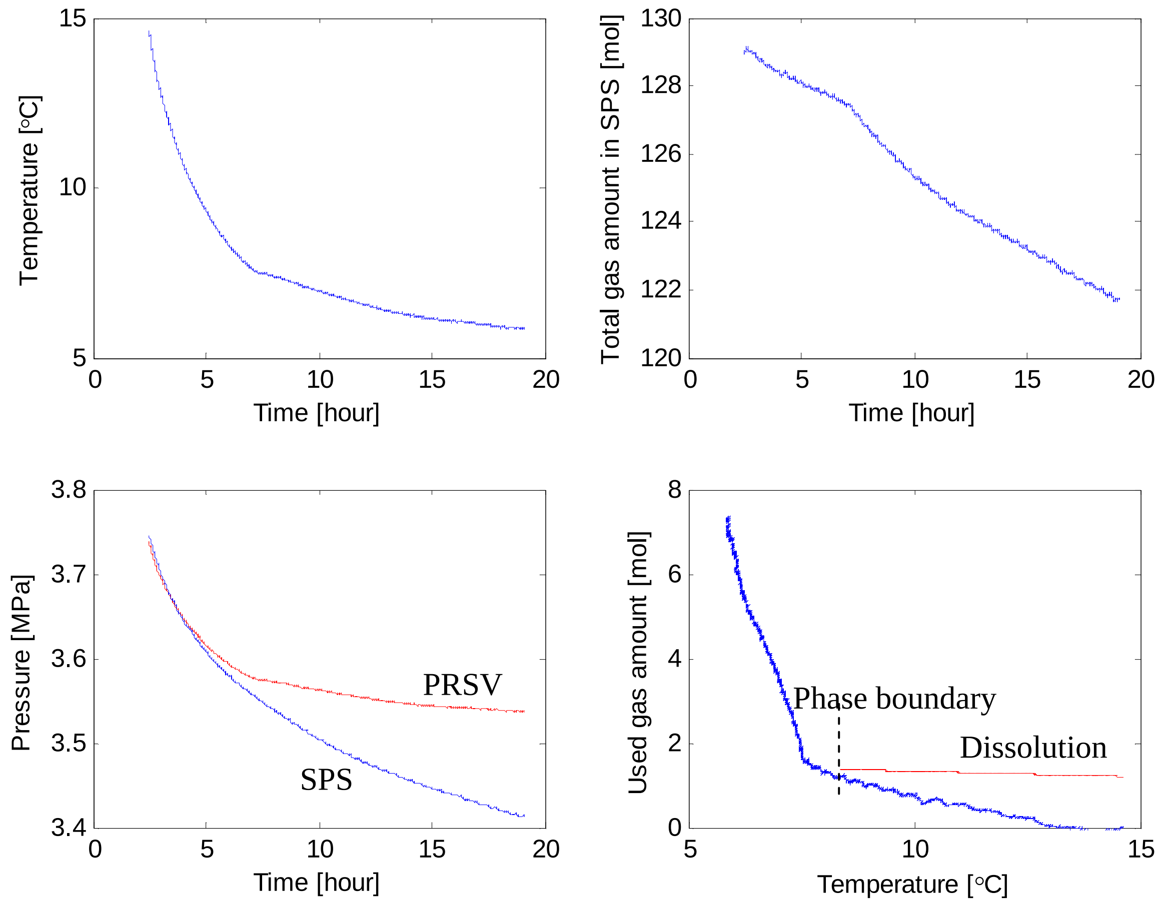

Figure 5. Calculation of the amount of gas converted to hydrate using the modified Peng-Robinson equation.

From the used gas amount (7.37mol), the amount of hydrate formed overnight can be estimated: 7.37 mol of hydrate in the case of zero solubility in water and 7.09 mol of hydrate when finite solubility is assumed, i.e., 1.233mol/kg from Duan group's calculator (http://www.geochem-model.org/models/h2o_co2/index.htm). Calculated hydrate saturation, i.e., $S_{hyd}=V_{hyd}/V_{void}$, is 35%.

Geophysical monitoring - Vs evolution

Shear wave measurements during hydrate formation/dissociation were also obtained as shown in the figures below:

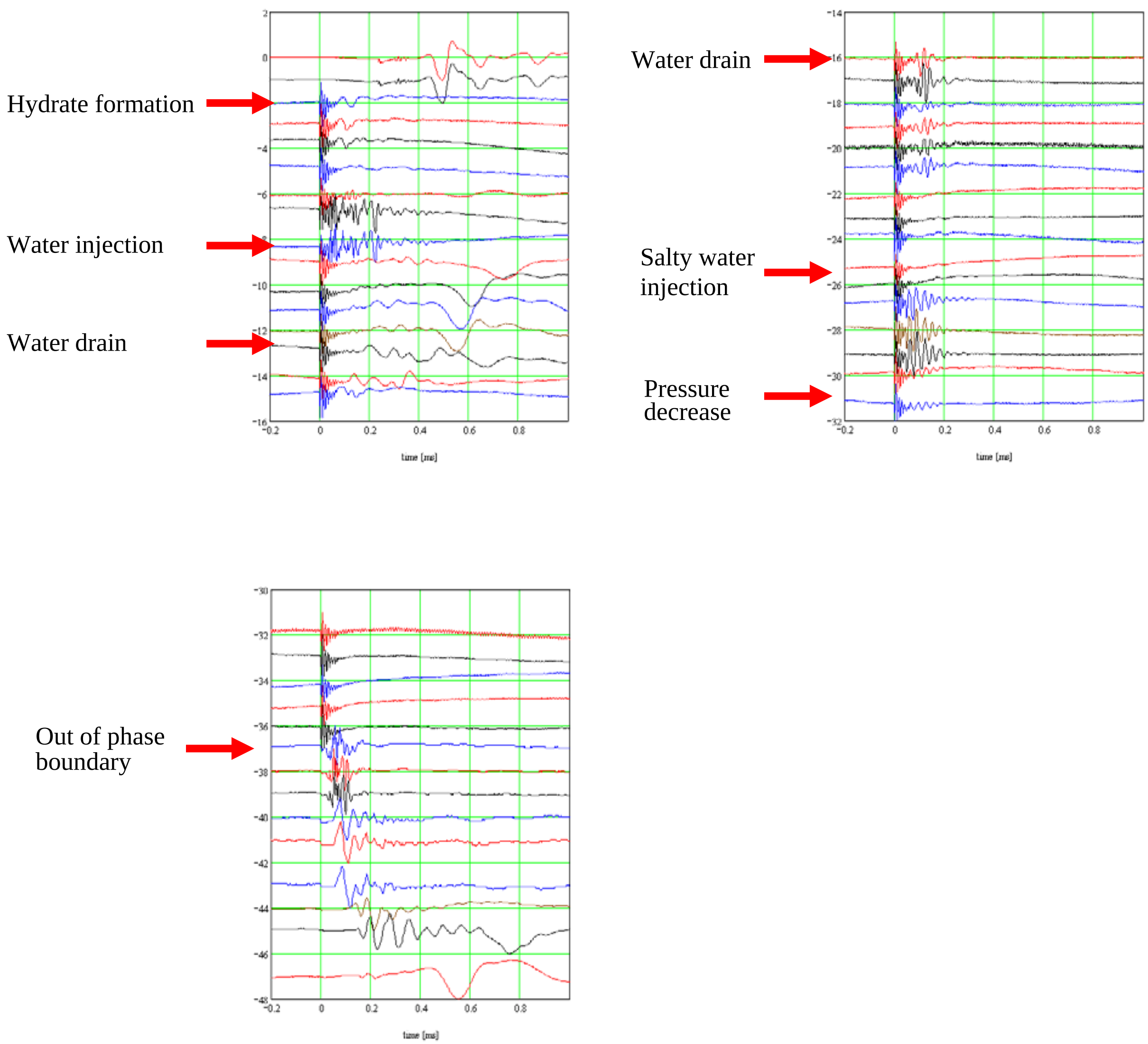

Figure 6. Shear-wave measurements were employed to detect hydrate formation.

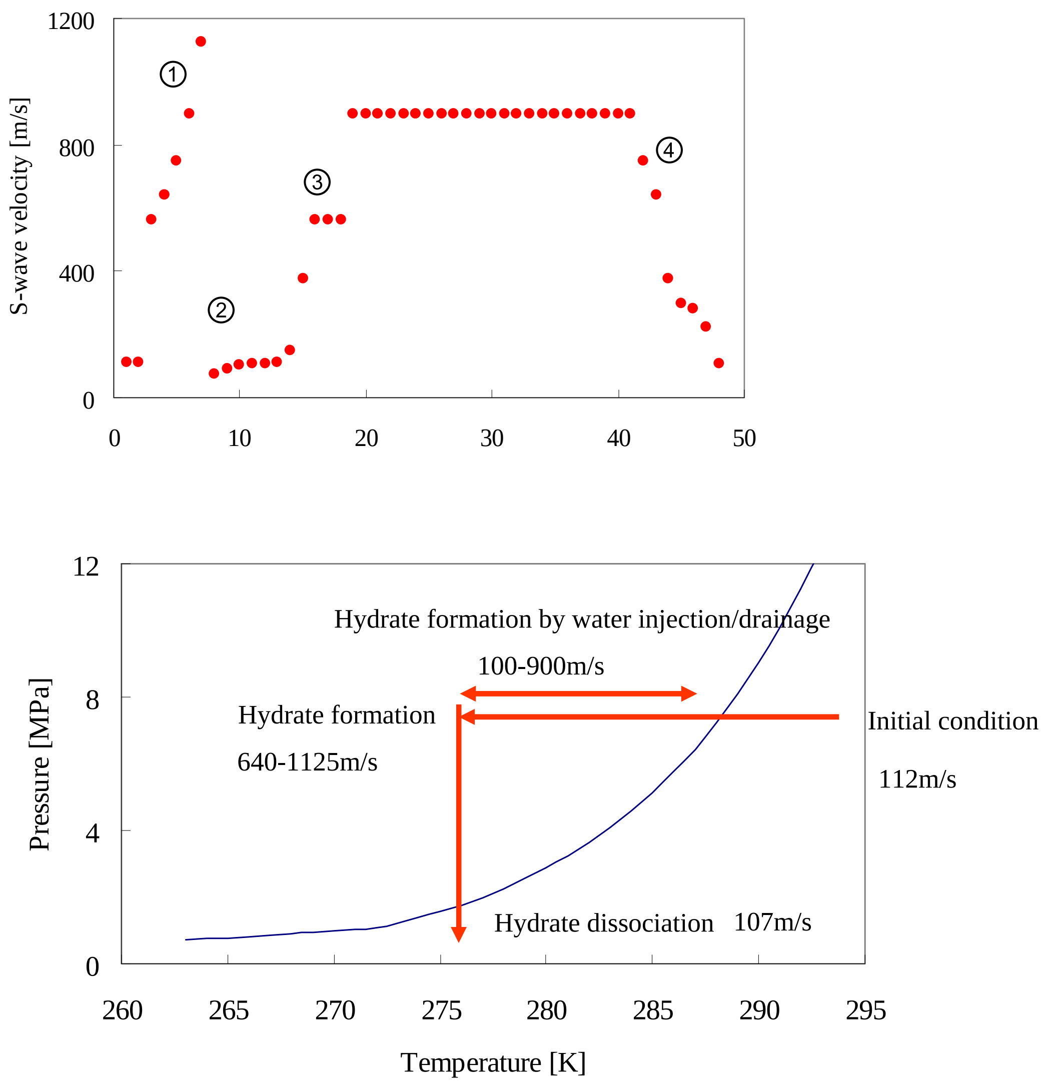

Figure 7. Shear-wave velocity measurements correlated with the phase diagram: ① Hydrate formation, ② Dissolution by water injection, ③ Hydrate formation by water drainage, and ④ Dissociation by depressurization

Note that the shear wave velocity increases during hydrate formation and decreases during dissolution and dissociation.

Post production fabric – Fine migration *(test #4)*
The sediment was split in six layers and sieved to identify trends in particle migration.
More fines were found in the upper part than in the lower part of the specimen. Apparently, fines from the lower part of the specimen migrated during the drainage through the hole of the chamber bottom. Fines also migrated and were produced out of the bottom plate during final depressurization. This behavior suggests that fines near a gas production point in a gas hydrate field will migrate with the water flow.

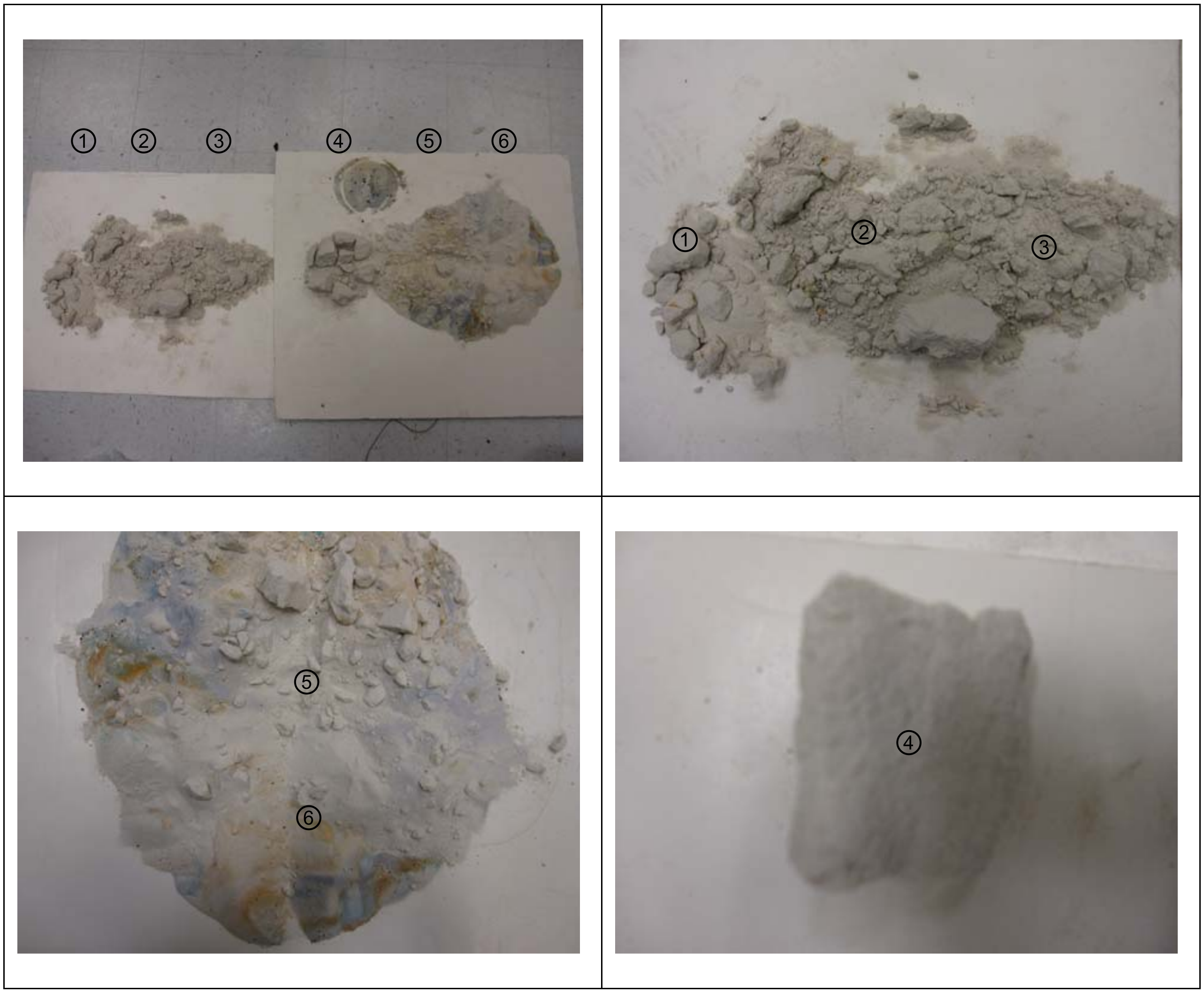

Figure 8. Sediment sampled after the experiment to determine the concentration of fine kaolinite particles along the test chamber: 1: top, 6: bottom.

Fine particle migration (test #4)

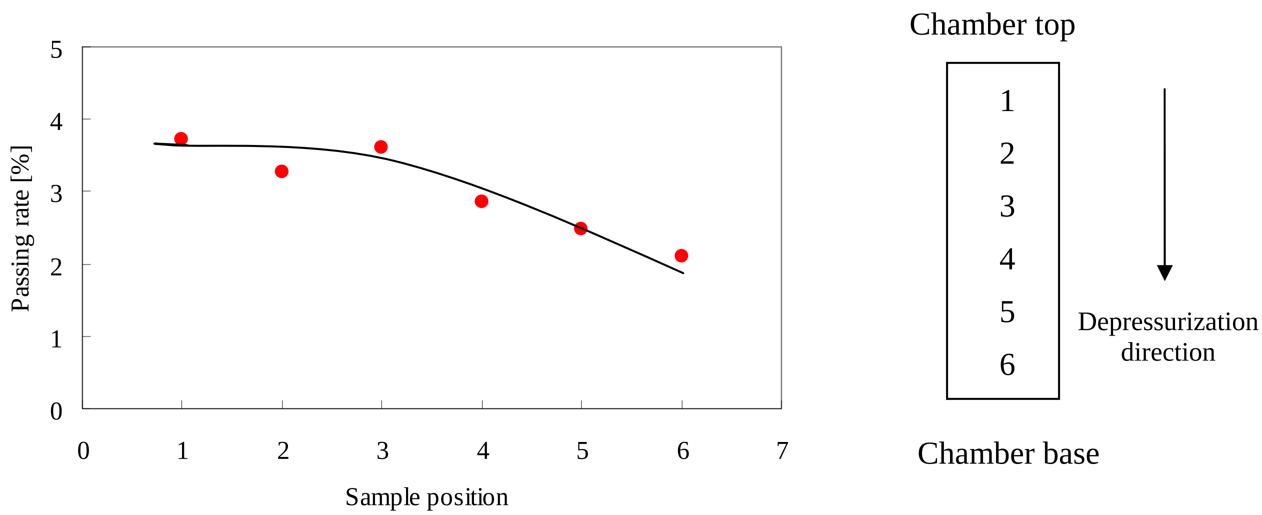

Figure 9. Distribution of kaolinite particles along the test chamber after the test.

A comparison of the results of Figure 9 with those reported earlier (Test 3 in Fall 2009 report) reveals some differences. For convenience, the results of Test 3 are shown in Figure 10 below:

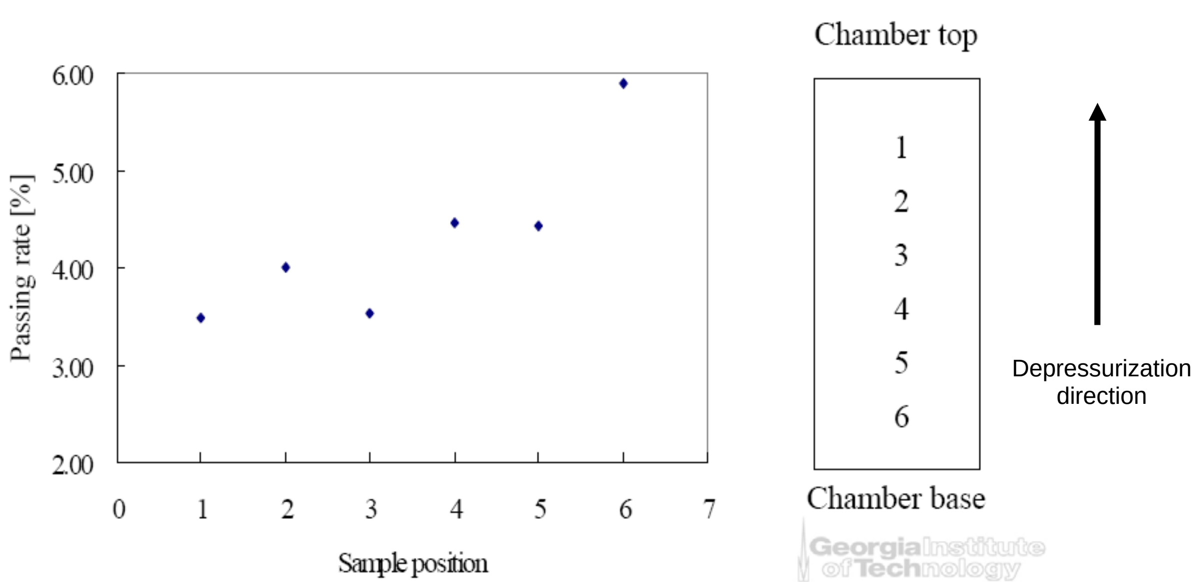

Figure 10. Distribution of kaolinite particles along the test chamber after Test 3.

The differences between Test 3 and Test 4 are the following:

1. In Test 4, a lower flowrate was used for fluid drainage, and depressurization occurred through the bottom of the vessel (instead of the top) at the end of the experiment.
2. Because of the low flowrate that was used for fluid drainage at the end of the test, no volume expansion, fluid-sediment instability, and fracture were observed in Test 4. These phenomena were observed in Test 3 where a higher flowrate was used for fluid drainage.
3. Less fines were found in the lower part than in the upper part of the specimen indicating that fines migrated with the flow during fluid drainage.

Conclusions

Based on Tests 1-4, the following conclusions can be drawn:

1. A water injection/drainage cycle stimulates hydrate formation in sediments
2. Hydrate dissociation occurs during water injection due to the solubility of gas in water
3. Shear-velocity measurements reveal qualitative hydrate formation/dissociation dynamics
4. Rapid gas production may cause clogging and sediment fracturing
5. Fluid drainage and depressurization lead to migration of fine particles
6. Avoiding migration of fines, clogging, and sediment instability during gas production will require controlling the fluid flowrate.